# Analysis of Higgs Boson Generation through Vector Boson Fusion in Proton-Proton Collisions at the Large Hadron Collider and its Interplay with Vector Boson Scattering

**Oscar Eatwell**

*Received March 22, 2025*
*Accepted June 22, 2025*
*Electronic access July 15, 2025*

We investigated the phenomena of Vector Boson Fusion (VBF) resulting in the production of a Higgs Boson. VBF occurs during proton-proton collisions in which two quarks radiate a W or Z (vector) boson each which then fuse into a Higgs boson, the quarks then form hadronic jets. We confirmed the topology and end states of such processes by simulating high energy collisions between protons at a centre-of-mass energy of 14 Tera electron-volts (TeV) in order to replicate the conditions of the Large Hadron Collider (LHC). We determined appropriate event selection cuts to accurately isolate VBF from its background processes. Finally, we analysed the interplay of VBF with Vector Boson Scattering (VBS) to identify appropriate event selection cuts for VBS. Our results allow us to be sensitive to these regions, which are in turn sensitive to Beyond the Standard Model (BSM) couplings. BSM theories are a group of models which include elements, such as additional particles, which are not in the Standard Model (SM) and have not been found experimentally yet. With our selection cuts, we obtained a signal efficiency of 73.8% for VBF and 56.1% for VBS while only 21% of background signals remained. We sought to quantify the effect of BSM physics on our kinematic observables, and determined that our selection cuts applied to VBF are sensitive to BSM physics for $c_{HW} > 0.001$ -the Wilson coefficient for H-W-W couplings.

## 1 Introduction

The Standard Model of Particle Physics (SM) is considered by many physicists as the most complete theory of physics, as it entirely describes our world as we know it. Four different categories of particles exist. First are leptons (such as electrons), next quarks (up quarks and down quarks for example), then boson's (such as Z or photons) and finally neutrinos (particles which have extremely low rates of interaction). They make up the basis of everything which surrounds us. These particles interact with each other due to four main forces mediated by their corresponding boson's. These forces include the electromagnetic, nuclear weak, nuclear strong and gravitational forces, although the latter is yet to be fully described by the Standard Model.[1–4]

Using particle accelerators such as the Large Hadron Collider (LHC) located near Geneva, physicists have been able to study the behaviour of fundamental particles at speeds approaching the speed of light when interacting between each other to better understand the Standard Model. Specifically, the LHC studies the fundamental properties of the Universe and the topology of the interactions which govern it by colliding energetic protons and analysing their decay products.

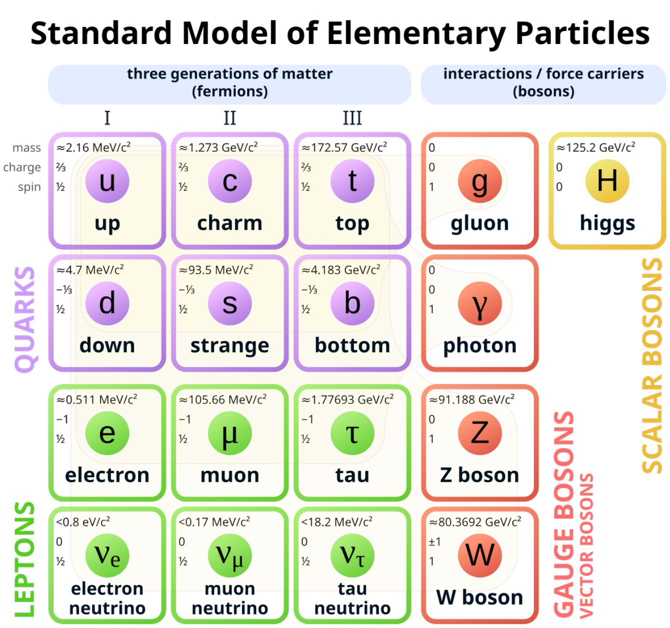


Figure 1: Diagram of the SM.

Since the inception of the LHC in 2008, particle physicists have made a multitude of groundbreaking discoveries. Many discoveries are centered around the Higgs mechanism. The Higgs mechanism can be considered aside from the rest of the

Standard Model due to its unique characteristics. The Higgs field dynamically generates the mass of particles which pass through it. It is thus responsible for the generation of the mass of fundamental particles besides the gluon and photon which are massless. Nonetheless, it is important to note that the Higgs field is only responsible for the generation of the mass of fundamental particles. The vast majority of the mass of baryons such as protons and neutrons is in the form of energy produced by the interaction of the strong nuclear force between quarks. As such, the Higgs field is only responsible for a small proportion of the universes total mass. The Higgs field extends across the whole known universe. The Higgs boson corresponds to an excitation of the Higgs field.

The ATLAS and CMS multipurpose experiments are large detectors at the LHC which investigate the Higgs mechanism and have made a slew of advances. Foremost is the experimental discovery of the Higgs boson in 2012 and the measurement of its mass at 125 GeV (GeV)[5,6], one of the primary goals for which the LHC was built. The Higgs bosons existence had previously been theorised by P. W. Higgs, F. Englert, R. Brout, G. S. Guralnik, C. R. Hagen, T. W. B. Kibble[7–12] in the 1960s. This discovery confirmed many theories surrounding the Higgs mechanism, since the Higgs boson is the physical manifestation of the mechanism behind it.

Theories confirmed include that the mass of particles is a result of the symmetry breaking of the electroweak (electromagnetic and nuclear weak) forces. Indeed, these forces initially have a symmetry which is broken by the Higgs field giving mass to the W and Z boson's while not affecting the photon. This allowed both the explanation of the origin of mass in the universe while also unifying the electromagnetic and weak forces at high energies. The ATLAS and CMS experiments continue their work notably by investigating in potential BSM theories, since many predict deviations in the Higgs Bosons mass, spin, parity or couplings due to this mechanism still being one of the least understood of the SM and the SMs strict restrictions notably regarding its couplings. Any deviations observed potentially in future ATLAS or CMS experiments, of parity, spin, decays or cross sections would suggest the existence of BSM physics.

The goal of our research is to obtain efficient selection cuts which could work simultaneously for VBF and VBS while retaining a discriminating factor, so that they are distinguishable from each other. Separately, we seek to model the effect of BSM physics on the observables of our experiment using EFTs.

We investigate the VBF production of the Higgs boson, as well as the role of the Higgs boson in VBS. VBF occurs during proton-proton collisions in which two quarks radiate a W or Z (vector) boson each which then fuse into a Higgs boson, the quarks then form hadronic jets. VBS occurs when the vector boson's do not fuse but rather scatter off each other by exchanging a virtual Higgs boson particle. We are analysing the $H$ (Higgs) $\rightarrow$ Z Z(Z boson-can be resonant or non-resonant) $\rightarrow 4l$ (lepton) $l = e$ (electron), $\mu$ (muon) decay channel. This refers to the Higgs bosons decay into two Z boson's which in turn decay each into lepton-antilepton pairs (electrons/positrons or muons/antimuons). The branching ratio of $H \rightarrow$ ZZ[13] is 2.6% and the Z $\rightarrow 2l$ is 6.73%[14].

Figures 1.2 and 1.3 are the Feynman diagrams of VBF and VBS, which show the evolution of particles over time:

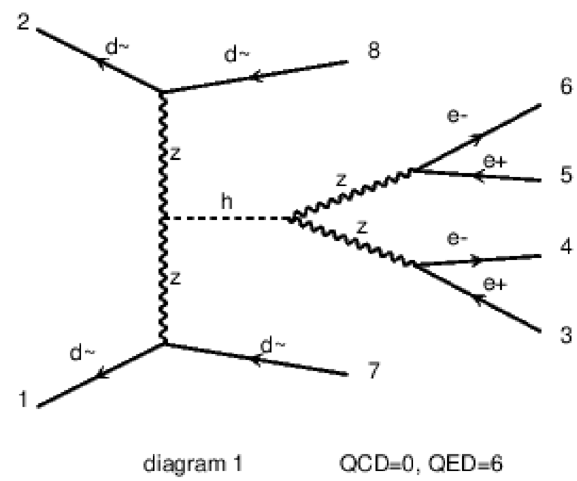


Figure 2: VBF Higgs production-Higgs boson is generated through fusion of vector boson's then decays following the $H \rightarrow ZZ \rightarrow 4l$ decay channel.

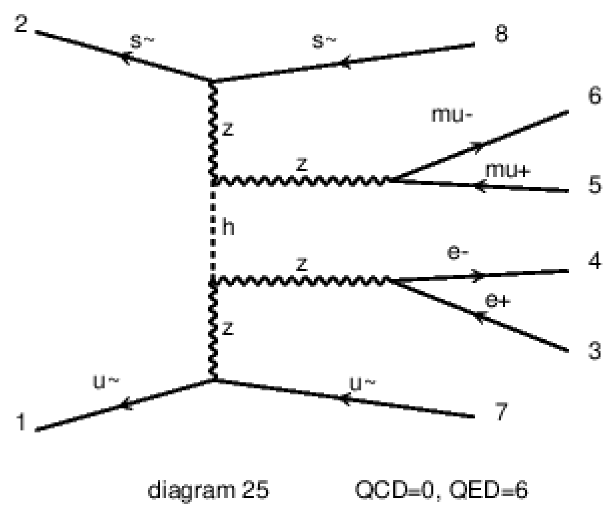


Figure 3: VBS Higgs virtual production- Z boson's scatter off each other by exchanging a virtual Higgs particle and then follow the $ZZ \rightarrow 4l$ decay channel.

 

Although these decays are relatively minor and are dominated by the $H \to bb$ (bottom quark) 58.2% branching ratio[13] and $Z \to bb$ 15.12% branching ratio[14], this decay is chosen due to its several advantages. Firstly, it is particularly interesting when analysing Higgs boson couplings to vector boson's since couplings occur both in the production and decay of the Higgs boson in VBF. It has also been a signature detection of the Higgs boson due to its relatively easy identification because of its clean final state and its very strong signal compared to its background[15].

Finally, since we are studying the VBS of two z boson's, the $H \to ZZ$ decay for VBF is strategic to analyse the interplay of VBF with VBS. Due to this decay channel, we make VBS and VBF have almost exactly the same production line. Indeed, the only difference between them is the production of an on/off shell Higgs depending on the process studied, allowing us to establish topological similarities more easily.

By analysing the couplings of the Higgs boson with vector boson's in both VBF and VBS, we could hypothesize the existence of BSM physics. This englobes all the theories which address some of the SM's issues, surrounding notably gravity, dark matter and matter-anti matter asymmetry. These include for example theories regarding the existence of extra dimensions.

The SM predicts very strict couplings between vector boson's and Higgs boson's, indicating that any divergences from such values would suggest errors within the SM. To do this though we must be able to isolate VBF and VBS signals.

Different models from effective field theories (EFT), which are BSM models, exist to take into account different values for couplings between the Higgs boson and vector boson's as well as the Higgs Boson coupling with itself.[15] Understanding both the VBF and VBS Higgs processes is thus extremely important in validating or disproving these theories, since multiple couplings between the Higgs Boson and Vector Boson's occur in these processes. If they are measured experimentally, we could gain insight on the validity of the SM. As such, establishing selection cuts to isolate VBF and VBS is necessary to conduct such an experiment at the LHC. To illustrate these EFTs, we are using simplified coupling models with simple coupling modifiers. Our objective is not to predict or measure the coupling values, but rather to isolate sensitive regions to these couplings and we are therefore not using full EFTs or even restricted models of EFTs.

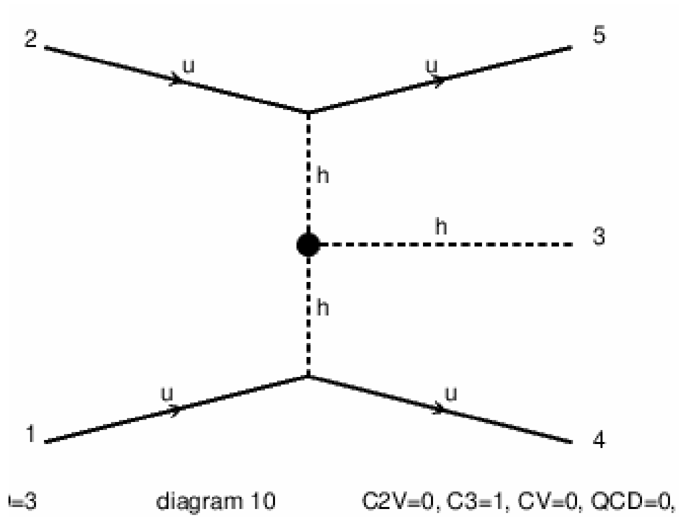


Figure 4: EFT Feynman diagram of Higgs boson coupling with itself.

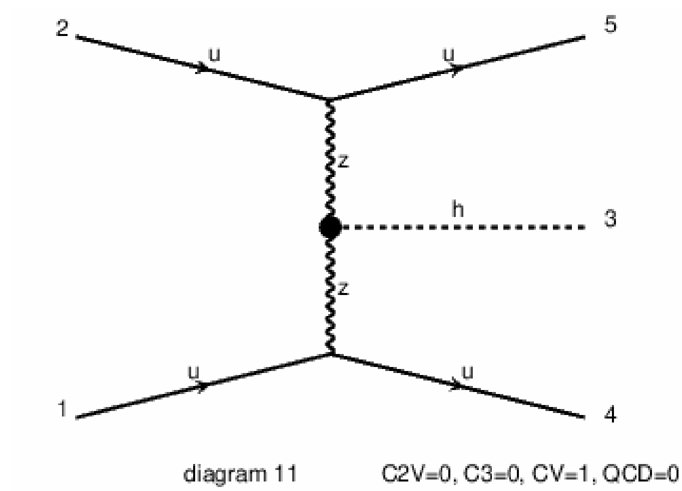


Figure 5: EFT Feynman diagram of VBF, Higgs boson coupling with vector boson's.

The circle at the vertices of these diagrams represents a different coupling value than that of the SM. The Goldstone equivalence theorem states that the scattering of VL VL to VL VL (with L being the longitudinal polarization of the vector boson V) is equivalent to the scattering of Goldstone Boson's. The Goldstone bosons play a role in the Higgs interactions[16]. This is why we see such vertices here. Flaws found in the SM could thus lead us to these EFTs, in which the Higgs boson does not behave exactly as predicted, as it couples differently than theorised by the SM.

These are just representations of EFT diagrams and are not representative of BSM models nor are they the focus of the study, which focuses on 13 TeV LHC collisions at lower energies than those where the Goldstone Boson's are involved. Measurements made at the LHC following our study could probe these theories however.

These are just representations of EFT diagrams and are not representative of BSM models nor are they the focus of the study, which focuses on 13 TeV LHC collisions at lower energies than those where the Goldstone Boson's are involved. Measurements made at the LHC following our study could probe these theories however.

Previous studies have sought to establish the topology and cross sections of both VBF and VBS. The fiducial cross-section of the VBF $H \to ZZ \to 4l$ decay channel was measured at $0.215^{+0.091}_{-0.076}$ fb[17] by the ATLAS collaboration. This experiment also helped establish topology and events selection cuts which will be confirmed and used in this paper to identify VBF. Nonetheless, it did not suggest the existence of BSM physics as it sought to test the CP-symmetry of the Higgs boson in order to explain the Universes baryon asymmetry. It however found a CP-even Higgs boson in conformity with the SM.

The CMS collaboration investigated the $H \to ZZ \to 4l$ decay channel without a focus on VBF and measured a fiducial cross section of 2.73fb[18], which correlates to SM predictions. This provides valuable insight on the decay channel we are studying. The CMS collaboration also conducted the first measurement of VBS involving di Z boson production, which helped characterize the topology of this key electroweak process and determined its fiducial cross section at $0.40^{+0.34}_{-0.25}$ fb[19], also consistent with SM predictions.

These studies have not, however, sought to investigate Higgs boson couplings with vector boson's by simultaneously or separately producing VBF and VBS signals. To prepare for such an experiment in the LHC which could suggest the existence of new physics, this investigation seeks to establish first the topology of VBF processes in order to establish appropriate event selection cuts to isolate the signal, then to determine whether such cuts could be applicable to VBS in order to simultaneously achieve pure VBF and VBS signals. This would allow the ATLAS or CMS experiments to measure coupling values specifically in relation to these processes, with the aim to clearly establish the coupling values between the Higgs boson and vector boson's. Measuring these values is essential to explore potential BSM theories.

In the next sections of this paper we will detail our methodology in gathering our simulated collision data. Next, we will present which events were selected and what are the background signals to VBF and VBS. Finally we will present our results and conclude on event selection cuts for simultaneous VBF and VBS analysis in regards to Higgs Boson generation.

# 2 Methods

## 2.1 Simulation

### 2.1.1 Event Generation

To simulate LHC collisions, we are using the MadGraph5 (MadGraph5_aMC@NLO)[20] software, which can model thousands of collisions simultaneously to gather representative data about a specific process. The software runs at Next-Leading Order (NLO) accuracy, which incorporates quantum effects to improve precision of results. We are generating our events at Leading-Order (LO) accuracy, which is sufficient to gather cross sections, invariant masses and angle distributions with high accuracy for the purpose of our experiment. Since in our analysis we are not seeking to make a specific very accurate measurement but rather identify parameters on which we can apply selection cuts to isolate Higgs couplings, we do not need to invest heavy computational resources in NLO. We generated 30,000 events for the VBF process, generated as:

$$pp > hjj$$

This represents a proton-proton collision which generates a Higgs boson and two jets. We decided to generate 30,000 events as this allows us to have a significant sample of events which satisfy our selection cuts, thus reducing the uncertainty of our results.

The VBS process with other electroweak lines of production with same end states included was generated as:

$$qq > zz\,jj\,\$\$h\,QCD = 0$$

This represents the interaction of two quarks producing two Z boson's and two jets without production of an on-shell Higgs, generated as 30 000 events in this case. It is important to note that due to the QCD=0, input we effectively remove any quantum chromodynamics (QCD) interactions which could pollute to purity of the VBS signal, preventing us from differentiating VBS from QCD $ZZjj$ events.

To determine if our event selection cuts were effective, we had to account for background processes such as gluon-gluon fusion (GGF), the leading production line of the Higgs boson, as well as single z production with two jets. We therefore produced 30 000 events for gluon-gluon fusion (a background signal to VBF) generated as:

$$gg > h\,QED <= 1\,[noborn = QCD] + gg > hjj \\ : QED <= 1\,[noborn = QCD]$$

This refers to the interaction of two gluons producing a Higgs boson and a Higgs boson with two jets through quantum chromodynamics and not quantum electro dynamics (QED).

 

Another background process generated was single z production with two jets, generated as:

$$pp > Zjj$$

Finally, the quantum chromodynamics (QCD) generation of two Z boson's and two jets, the main background signal to VBS was simulated as:

$$pp > ZZ\,jj\,QCD^2 == 2$$

This refers to a proton-proton collision forming two z boson's and two jets through quantum chromodynamics. To verify this process does involve QCD diboson production, we generated Feynman diagrams of the process, one of which was:

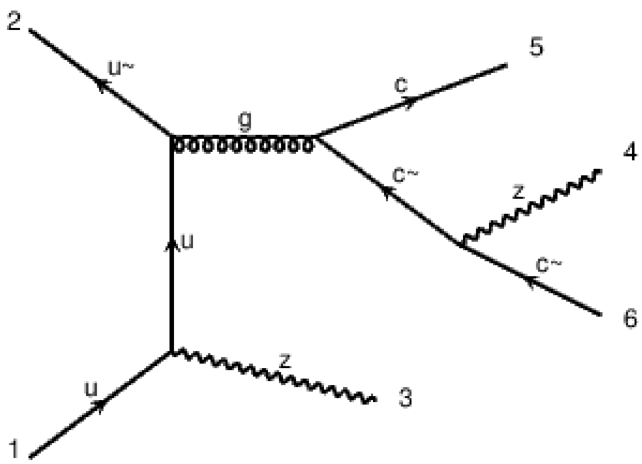


Figure 6: Di Z Boson and dijet production through QCD, a background to VBS.

We used the Pythia8[21] Monte Carlo event generator to simulate parton showering and decays. Parton showering simulation allows quarks to convert into hadronic jets which are part of the final state of the processes we are analysing.

This simulation takes into account the near infinite array of radiations and decays which can happen within a hadronic jet. This is important since leptons can be produced by hadronic jets and be part of the final state of an event, thus influencing our event selection. Pythia8 is also used to decay particles appropriately to achieve similar final states so as to analyse each process more effectively. For instance, since we are making use of the $H \to ZZ \to 4l$ decay channel, Pythia8 is used in all events to decay a Higgs boson into two Z boson's and subsequently each Z boson is decayed into a lepton-antilepton pair. This allows us to obtain a maximum number of results which conform to our decay channel.

#### 2.1.2 Background

In this section we discuss background events. Background events are the processes which have similar topologies to the process we are studying, the signal, which prevents us from differentiating them easily. In the case of VBF, its background would be a process which involves on-shell Higgs Boson generation and can result in its decay into two vector boson's and finally four leptons.

Background events are taken into account and generated, in order to identify what cut offs effectively isolate the VBF and VBS signals from their background. These are regions sensitive to BSM models with different Higgs boson coupling values, and thus are important to study. The first background process for VBF is gluon-gluon fusion (GGF), which is the leading line of production of the Higgs boson at a cross section of 48.6pb[22] which would easily overpower the VBF signal of only 3.766 pb[23]. The background process for VBS is the QCD production of two jets and two Z boson's, since VBS has the same end states but does not entail the QCD interactions. Finally the production of a Z boson with two jets is also taken into account with both its decay into one and two lepton-antilepton pairs. According to our results this specific process was extremely minor and is thus negligible, although it is nonetheless included in the simulation.

#### 2.1.3 Detection

Delphes[24] is a computational framework which is an efficient and parameterized detection simulator. This virtual detector realistically reproduces how particles emitted in final states interact physically with a detector and reconstructs such particles into observables. These include discussed particles such as leptons, jets and boson's. Despite having a lower accuracy than full scale slower detection simulators such as GEANT4[25], Delphes nevertheless allows for investigations in BSM physics. Using Delphes rather than GEANT4 does increase the uncertainty of our results. However, since we are not attempting to make an exact measurement, but rather quantify an overall efficiency, Delphes is sufficient. Delphes simulates the actions of detection instruments such as trackers, and both electromagnetic and hadronic calorimeters. It takes into account actual imperfections observed at the LHC such as slightly flawed trigger efficiencies and difficulties in differentiating particles situated very close to one another.

When multiple collisions happen simultaneously, pile-ups are also simulated using the Delphes software. This detection allows us to effectively simulate an ATLAS or CMS detector in order to gather data on reconstructed events, such as invariant mass, transverse momentum, or pseudo rapidity values of observables used later on to analyse processes using the ROOT scripts in C++. ROOT is a framework developed by CERN which Delphes relies on to provide statistical data regarding a collision which is used in our analysis. Our scripts using ROOT which interpreted Delphes detector results allowed us to determine appropriate event selection cuts to isolate VBF and VBS.

### 2.2 Event Selection

In regards to lepton analysis, events are selected if they contain at least four leptons in the final state, composed of at least two oppositely charged same flavour leptons. Leptons must also satisfy the criteria: transverse momentum ($p_t$) $> 5$ GeV. Transverse momentum is the momentum of a particle perpendicular to the beams axis, which is the z axis. We are using this selection cut as often, in real-world scenarios, particles with $p_t < 5$ GeV are difficult to reconstruct properly, and we are seeking to emulate reality.

All possible pairs are computed and the pair of leptons whose invariant mass is closest to the mass of the Z boson (91.2 GeV)[26] is selected and labelled as the leading dilepton. The leading dilepton is followed by the sub-leading dilepton, whose invariant mass is the second closest to 91.2 GeV. The invariant mass of the quadrivectors of the four leptons is then calculated, with cuts integrated for 105-160 GeV and a more aggressive one at 110-130 GeV to identify presence of an on-shell Higgs Boson, whose mass is 125 GeV.

Events are also selected based on jet reconstruction. Events must have at least two jets, which both satisfy the criteria $p_t > 25$ GeV. The decision of this selection cut is for the same reason as the lepton cut on $p_t$. Jets are then ordered based on their $p_t$, with the jet with the most $p_t$ first. The jet with the most $p_t$ is labelled as the leading jet, followed by the sub-leading jet with the second-most $p_t$. The difference between the leading and sub leading jets pseudo rapidity ($\Delta\eta_{jj}$) is calculated. Pseudo rapidity ($\eta$) is related to the polar angle formed between the particles trajectory and the beams z axis. Pseudo rapidity is thus an indicator of the angle of the trajectory of a jet. A high $\Delta\eta$ value thus signifies jets with different trajectories.

The invariant mass of the two jets is also calculated. Cuts are applied for $|\Delta\eta_{jj}|$(difference of pseudo rapidity of two jets)$>$ 2.5 and $m_{jj}$ (mass of two jets) $> 200$ GeV. This is due to the particular topology of VBF, which is detailed in the results section. Specifically, for the VBF process generation, cuts are preemptively applied for $|\Delta\eta_{jj}| > 0.5$ and $m_{jj} > 150$ GeV to remove parasite events due to bugs in the MadGraph5 software and improve the purity of the VBF signal.

| Selection Cut Description | Quantitative parameter cut |
|---|---|
| Minimum dijet $p_t$ | $p_t > 25$ GeV |
| Jet selection cuts | $|\Delta\eta_{jj}| >2.5$ and $m_{jj} > 200$ GeV |
| Lepton Range cut | $110 < m_{l+l-l+l-} < 130$ GeV |
| Extended Lepton Range cut | $105 < m_{l+l-l+l-} < 160$ GeV |

**Table 1** Summary of the event selection cuts we used and are investigating.

## 3 Results and Discussion

In this section we discuss the results obtained from our research. We generated graphs using the ROOT framework with C++ scripts. The results are presented below.

### 3.1 Topology of Vector Boson Fusion

In this section we study the defining characteristics of VBF: its topology. We seek to identify parameters which are unique to VBF and could serve to differentiate it from its background using event selection cuts.

#### 3.1.1 Mass of four Leptons

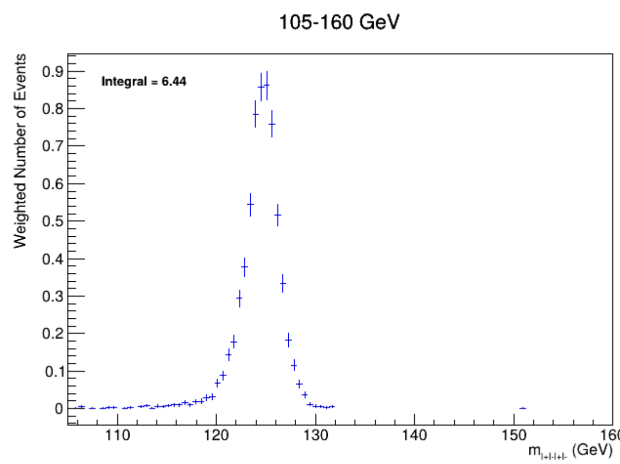


Figure 7: Number of weighted events measured in relation to invariant mass of four leptons for VBF. Weighted events reflect the number of actual events one would get at an LHC run, in this case at $\mathscr{L} = 139\text{fb}^{-1}$.

Our first objective was to confirm the topology of the VBF process. That is its defining characteristics, identified through various metrics such as invariant masses of both leptons and jets as well as pseudo rapidity $\eta$ values. Our first conclusion is that, as expected, VBF is resonant with the Higgs boson and thus the invariant mass of the four leptons emitted from VBF peaks at 125 GeV.

The distinct peak at 125 GeV for the invariant mass of the four detected leptons, as seen in Figure 7, is thus a characteristic of the topology of the VBF process. This proves that VBF produces an on-shell resonant Higgs boson.

#### 3.1.2 Pseudorapidity

The VBF signal produces two characteristic jets, often with accentuated angles for the forward jets, that is the jets with the most $p_t$. We establish that the leading jets of VBF have high $\Delta\eta$ values. The number of events peak at $\Delta\eta$ values of around 4 and -4 as shown in Figure 8. These values suggest that the forward jets produced by VBF spread far apart in different directions.

 

Parity (CP) violation in VBF.[17]

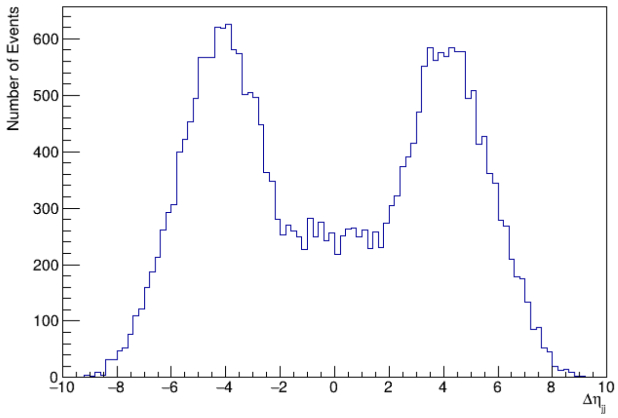


Figure 8 Number of events measured in relation to $\Delta\eta$ of the two leading jets for VBF.

Separated forward jets characterised by high $\Delta\eta$ values which form two distinct peaks thus are part of the topology of VBF.

The $\Delta\eta$ of the two leading jets is also related to their mass, with particularly large concentrations of high mass jets with large $\Delta\eta$ values.

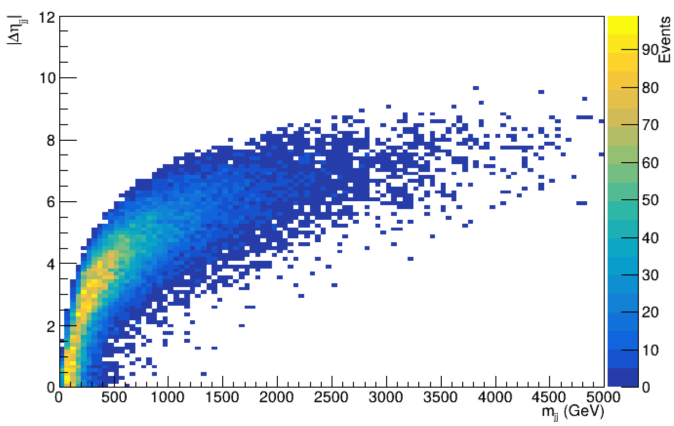


Figure 9 $|\Delta\eta|$ of two leading jets for VBF in relation to their invariant mass.

As shown in Figure 9, VBF has a wide range of jet masses from close to 100 GeV to 5000 GeV, with large numbers of events at relatively high energy levels such as 500 GeV. Pseudo rapidity increases starkly at first as mass of jets increase. This, however, levels off, although a significant number of events are detected beyond energies of 1000 GeV. As such, the two leading jets which make up VBF processes often have high $|\Delta\eta|$ and high invariant masses.

The ATLAS experiment found a similar kinematic distribution when measuring these parameters in search of potential Charge-Parity (CP) violation in VBF.[17]

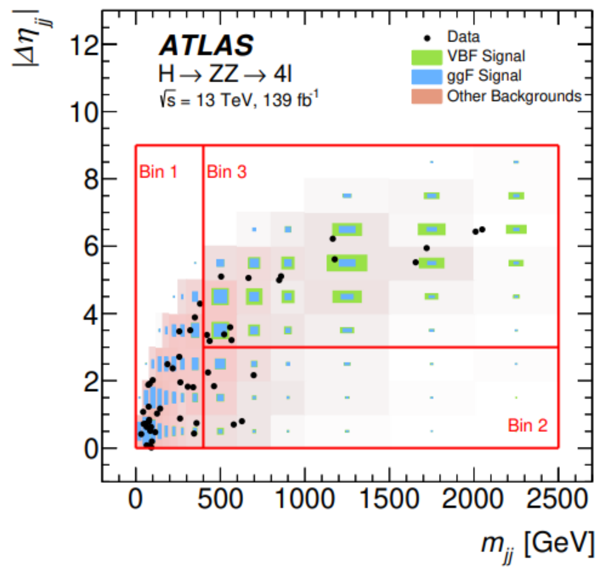


Figure 10 $|\Delta\eta_{jj}|$ and $m_{jj}$ kinematic distributions obtained experimentally by the ATLAS experiment's search.[17]

This distribution follows the same pattern as ours. As such, experimental data validates our simulation model.

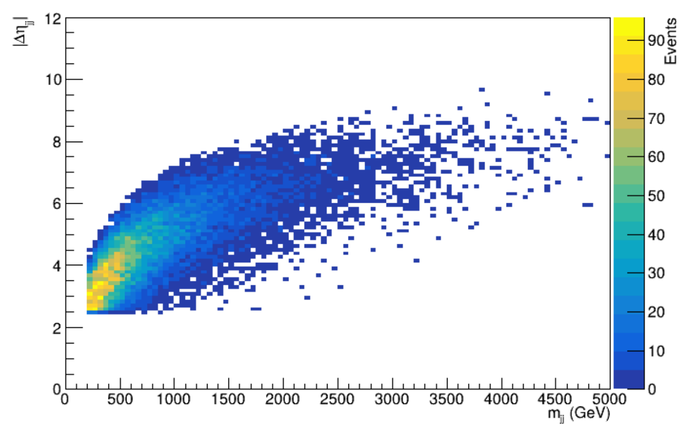


Figure 11 $|\Delta\eta|$ of two leading jets for VBF in relation to their invariant mass after selection cuts $|\Delta\eta_{jj}| > 2.5$ and $m_{jj} > 200$ GeV.

Due to VBFs high $|\Delta\eta_{jj}|$ and $m_{jj}$, chosen selection cuts, $|\Delta\eta_{jj}| > 2.5$ and $m_{jj} > 200$ GeV, minimally affect the number of VBF events generated as shown in Figure 11. These cuts can therefore be used to remove the signals background and improve purity of signal.

### 3.2 Events after Selection Cuts

The identified topology of VBF can be used to isolate it from its background in future LHC runs by applying identified selection. These selection cuts also allow comparison between the topology of VBF and the topology of its background processes, as well as allow establishment of whether VBF and VBS can be run simultaneously with identical selection cuts.

#### 3.2.1 Gluon Gluon Fusion

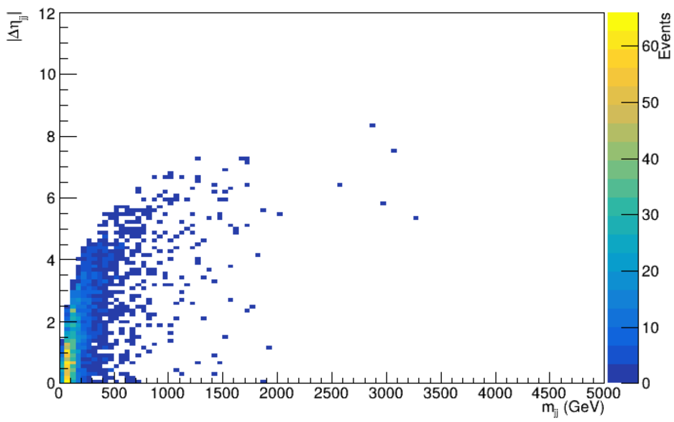


Figure 12 $|\Delta\eta|$ of two leading jets for GGF in relation to their invariant mass.
top) Before selection cuts
bottom) After selection cuts $|\Delta\eta_{jj}| > 2.5$ and $m_{jj} > 200$ GeV

GGFs topology shares similarities with that of VBF but has distinct differences. Just like VBF, the invariant mass of the four leptons issued from GGF peaks also around 125 GeV, as shown in Figure 13, since GGF produces an on-shell resonant Higgs boson.

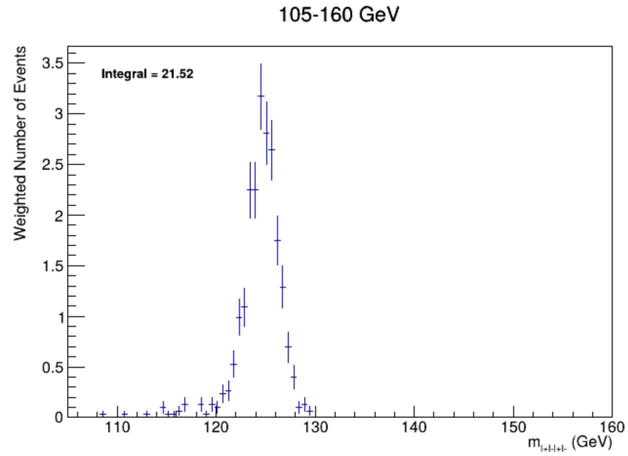


Figure 13 Number of weighted events measured in relation to invariant mass of four leptons for GGF.

Nonetheless, the jets resulting from GGF are extremely different from those produced through VBF. Indeed, as shown in Figure 12, $|\Delta\eta_{jj}|$ values tend to reach a maximum around 5, and events are largely concentrated around $|\Delta\eta jj| = 1$. This shows that the leading jets of GGF are much closer together and have similar directions. Their masses are also much smaller than those of VBF, barely going past 500 GeV as opposed to the 1000 GeV of VBF. Therefore, although cuts on the invariant masses of leptons are inefficient to remove GGF from a signal since it produces an on-shell resonant Higgs boson, cuts on $|\Delta\eta_{jj}|$ and $m_{jj}$ are effective in almost suppressing GGF while preserving VBF, thus improving the purity of a signal, as demonstrated by Figure 12. Overall GGF has a very different topology to VBF, which allows us to effectively cut it out.

#### 3.2.2 Vector Boson Scattering

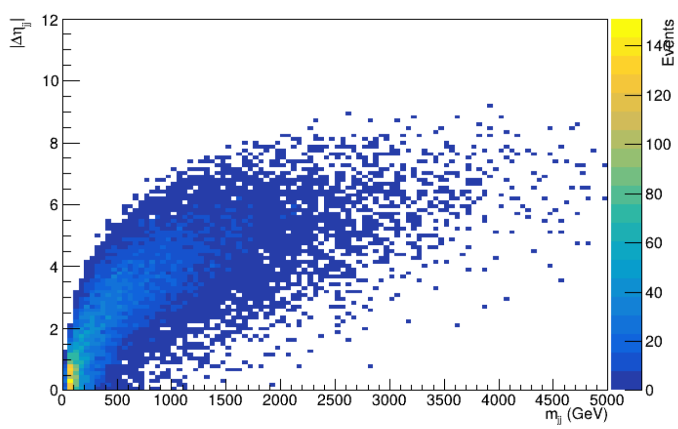

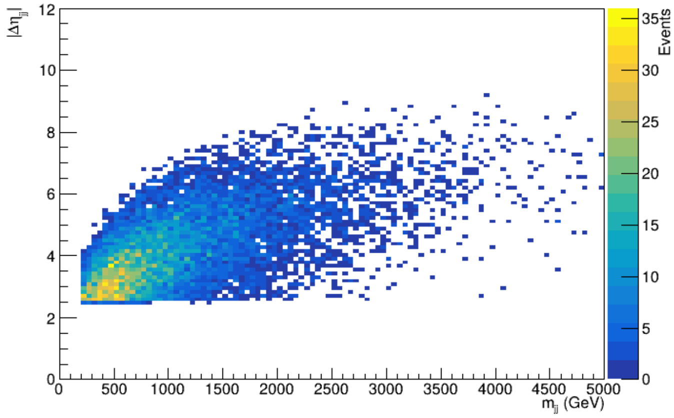


Figure 14 $|\Delta\eta|$ of two leading jets for VBS in relation to their invariant mass.
top) Before selection cuts
bottom) After selection cuts $|\Delta\eta_{jj}| > 2.5$ and $m_{jj} > 200$ GeV

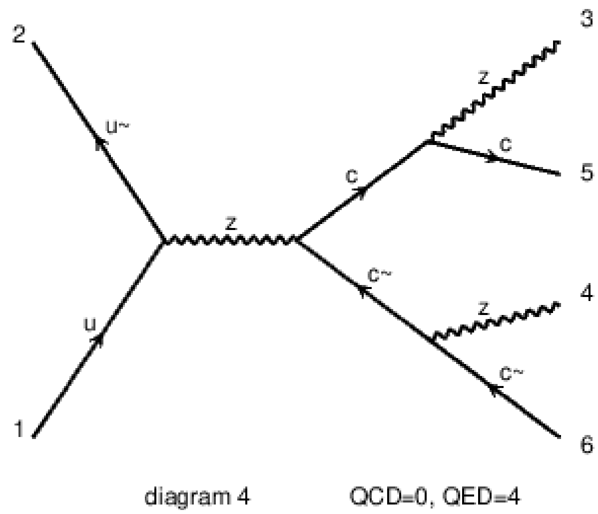


Figure 15 Two quarks fuse into a Z boson which then decays into a set of jets which radiate two Z boson's.

VBS has a wider spread for $|\Delta\eta_{jj}|$ and $m_{jj}$ than GGF and resembles closely the VBF signal in its spread, indicating clear topological similarities. As shown in Figure 14, $|\Delta\eta_{jj}|$ are concentrated around low values but spread wide with many events with $|\Delta\eta_{jj}| > 4$, $m_{jj}$ values go beyond 1000 GeV in many cases. As seen on Figure 14 many events remain despite the selection cuts, just like the VBF signal. Although there are topological similarities between VBF and VBS, it is important to note that VBF and VBS have clear topological differences. Indeed, VBF involves the production of an on-shell Higgs Boson while VBS is mediated by off shell Higgs exchanges and quartic gauge couplings at WWZZ vertices for example.

Our selection cuts therefore evidently allow simultaneous running of VBF and VBS, since a large portion of both the VBS and VBF signals are preserved after their implementation. Nonetheless, the cut is not perfect, as a considerable part of the signal is cut off. This, however, could be due to the fact that our VBS signal includes other electroweak interactions other than VBS itself. We might therefore be cutting out background to VBS, since many other electroweak interactions can potentially produce two Z boson's and two jets in the final state. An example Feynman diagram of such a hidden background is: The perceived reduction of the strength of the VBS signal induced by the cut could in fact be purifying it from additional hidden background events. This, however, is not certain and must be further investigated. Overall, though, we can conclude that the jets resulting from VBS have a very similar topology to those resulting from VBF.

Besides, separately we discovered that there are no events in which the invariant mass of four leptons is in between 110 and 130 GeV within our limit of 8295 events. Which demonstrates that VBS does not produce a resonant Higgs boson as expected. This allows us to discriminate between VBF and VBS if we wish to study their signals separately. A restriction of the invariant mass of four leptons between 110 and 130 GeV would remove the VBS signal while a suppression of all such events would remove the VBF signal. We can thus both simultaneously and separately analyse VBF and VBS.

#### 3.2.3 Quantum Chromodynamics di Z Boson and dijet line of production

As shown in Figure 16, the background to VBS has much more condensed $|\Delta\eta jj|$ and $m_{jj}$ values. As such, our cut on $|\Delta\eta_{jj}| > 2.5$ and $m_{jj} > 200$ GeV greatly improves our signal to background ratio for VBS. It successfully removes the majority of the QCD background signal events while preserving much of the VBS signal. Considering QCD diboson dijet production is the main background process to VBS, this allows us to effectively isolate VBS.

Besides, we discovered separately that there are no results for a restriction on the mass of leptons for 110-130 GeV within our limit of 30,000 events. Therefore, the signal can completely be eliminated though by a cut on the invariant mass of leptons of 110-130 GeV, since there is no resonant Higgs boson's production.

### 3.3 Overall efficiency of event selection cuts

The cuts $|\Delta\eta_{jj}| > 2.5$ and $m_{jj} > 200$ as well as $110 < m_{l+l-l+l-} < 130$ GeV allow us to simultaneously isolate VBF and VBS signals very efficiently, while retaining the ability to analyse them together. As seen on the efficiency table in Ta-

| Process | VBF | VBS | GGF | QCD VBS Background |
|---|---|---|---|---|
| Two jets | 477636.89 ±2250.1 | 18855.42 ±32.0 | 1152414.51 ±1390 | 336775.34 ±597.7 |
| $\lvert\Delta\eta_{jj}\rvert$ $m_{jj}$ cuts | 352665.63 ±1662.0 | 10579.85 ±18.0 | 250049.72 ±301.6 | 71061.46 ±126.1 |
| 4l in final state | 6.48 ±0.21 | 11.43 ±0.01 | 21.72 ±0.1 | 169.25±2.2 |
| 4l (110-130 GeV) | 6.41 ±0.21 | 0 ±0 | 21.49±0.1 | 0.13±0 |
| 4l (105-160 GeV) | 6.44 ±0.21 | 0.01 ±0 | 21.52±0.1 | 0.54±0 |

**Table 2** Number of weighted events at luminosity $\mathscr{L} = 139\text{fb}^{-1}$ for each process for all cuts. Weighted events at this luminosity reflect the number of events obtained during a real LHC experiment. They reflect the cross section of the event rather than the number of events generated.

| Process | VBF | VBS | GGF | QCD VBS Background |
|---|---|---|---|---|
| $\lvert\Delta\eta_{jj}\rvert$ and $m_{jj}$ | 73.8±0.49 | 56.1±0.13 | 21.7±0.04 | 21.1±0.05 |
| Lepton (110-130 GeV) | 98.9 ±4.56 | 0±0 | 98.9 ±0.65 | 0.08 ±0 |
| Lepton (105-160 GeV) | 99.4 ±4.56 | 0.09 ±0 | 99.1 ±0.65 | 0.32 ±0 |

**Table 3** Calculated percentage cut efficiencies for each process

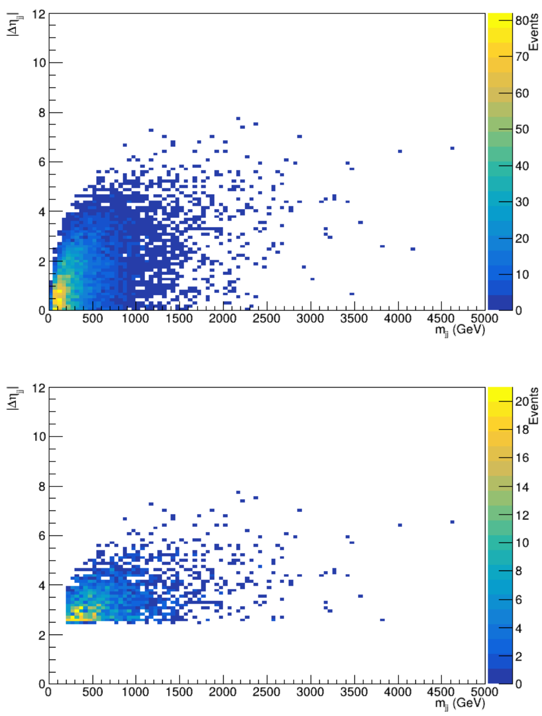


Figure 16 $|\Delta\eta|$ of two leading jets for QCD di Z boson production in relation to their invariant mass.
top) Before selection cuts
bottom) After selection cuts $|\Delta\eta_{jj}| > 2.5$ and $m_{jj} > 200$ GeV

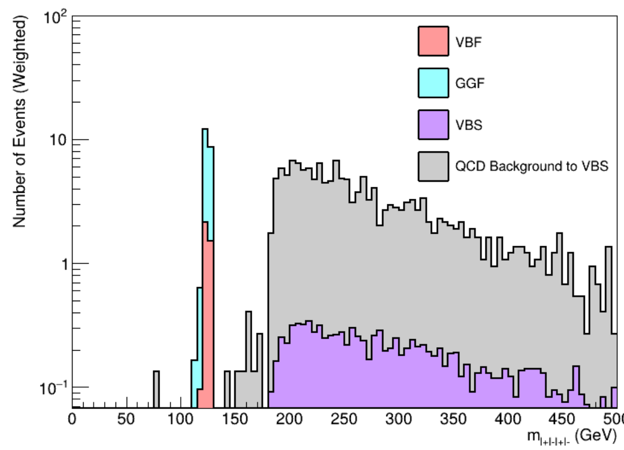


Figure 17 $m_{l+l-l+l-}$ distributions for each process studied, events are weighted an thus reflect the cross section of each process.

ble 3, 73.1% of the VBF signal is preserved by our cuts and 56.3% of the VBS signal is also kept when disregarding lepton range. On the other hand, almost 80% of background events such as GGF and QCD $zzjj$ productions are cut out. As such, our selection cuts allow us to reduce the original 1:2.4 signal-to-background ratio for VBF to a 1:0.7 signal-to-background ratio. Separately, these cuts allow us to reduce the original 1:18 signal-to-background ratio for VBS to a 1:7 signal-to-background ratio. It is therefore possible to run a single experiment at the LHC examining both VBF and VBS.

Moreover, we can also singularly isolate VBF and VBS if we wish to study these processes separately. Indeed, we can obtain a very pure VBF signal by using the $|\Delta\eta_{jj}| > 2.5$ and $m_{jj} > 200$ GeV cuts while adding the cut for $110 < m_{l+l-l+l-} < 130$ GeV. This effectively removes VBS and the QCD di Z boson dijet production line, since 0% of their signals remain after that the $110 < m_{l+l-l+l-} < 130$ GeV cut, while retaining a 1:0.7 signal to background ratio for VBF, allowing us to single out VBF. This is evidenced in Table 3 under the "Efficiency of cuts within lepton range" column.

On the other hand, we can isolate VBS, although the signal will be a little less pure than that of VBF, by using the $|\Delta\eta_{jj}| > 2.5$ and $m_{jj} > 200$ GeV cuts while adding a cut retaining only signals outside of the lepton range $110 < m_{l+l-l+l-} < 130$ GeV. This removes VBF as well as GGF completely as seen in Table 3 under the "Efficiency of cuts outside lepton range" column, as 99% of their signal lies within it and therefore only 1% outside. This is also seen in Figure 17, where VBF and its background and VBS and its background have distinctly separate $m_{l+l-l+l-}$ values, as VBF is resonant at 125 GeV while VBS is at around 180 GeV (the mass of two Z boson's). As such, simultaneous and separate analysis are both possible.

Simultaneous analysis would provide more instances of Higgs to vector boson couplings, giving a larger data set to work with but a higher uncertainty due to more background events such as GGF and the QCD background to VBS. Combined analysis would also allow further topological comparison between VBS and VBF. Separate analysis, despite giving a more restricted dataset, would allow a more certain measurement.

### 3.4 Sensitivity of Selection Cuts to BSM physics

We sought to explore how sensitive our event selection cuts would be to BSM physics. We used the Higgs effective Lagrangian (HEL), an EFT framework, which models the potential effects of BSM physics. This is the Lagrangian of the HEL framework:

$$\mathscr{L}_{\text{HEL}} = \mathscr{L}_{\text{SM}} + \sum_i \frac{c_i}{\Lambda^2}\mathscr{O}_i$$

Where $\mathscr{L}_{\text{HEL}}$ is the HEL Lagrangian, $\mathscr{L}_{\text{SM}}$ is the SM Lagrangian, $c_i$ are Wilson coefficients, $\mathscr{O}_i$ are dimension six operators and $\Lambda$ is the high-energy cut off typically around 1 TeV. We modified the $c_{HW}$ Wilson coefficient while keeping the other coefficients at 0, thus adding the term:

$$\frac{c_{HW}}{\Lambda^2}\mathscr{O}_{HW}$$

to the SM Lagrangian. This addition modifies the kinetic structure of the H-W-W vertex, which is part of HVV couplings, an important part of VBF. This modification does not emulate any specific BSM theory, but rather a general consequence of BSM physics. We calculated the standard deviation between the number of BSM VBF events and SM VBF (for $c_{HW} = 0$) events passing our event selection cuts to determine the sensitivity limit of our selection cuts to BSM physics using the formula:

$$Z = \frac{N_{\text{BSM}} - N_{\text{SM}}}{\sqrt{N_{\text{SM}}}}$$

The uncertainty at values below $c_{HW} = 0.001$ is too large to draw conclusions on. However, for $c_{HW} > 0.001$, standard deviation exceeds $3\sigma$, even taking uncertainty into account, which corresponds to a confidence level of 99.7%. The sensitivity limit on H-W-W couplings of our selection cuts for the VBF process is therefore $c_{HW} = 0.001$ at 99.7% confidence.

| $c_{HW}$ | Number of events passing cuts (VBF) | Z |
|---|---|---|
| 0 | $218461.78 \pm 1390$ | 0 |
| 0.0001 | $219822.8 \pm 1282.7$ | $2.91 \pm 2.74$ |
| 0.0003 | $220098.63 \pm 1529$ | $3.50 \pm 3.27$ |
| 0.001 | $217271,38 \pm 1306.6$ | $-6.03 \pm 2.80$ |
| 0.01 | $207945,59 \pm 1306.6$ | $-20.01 \pm 2.80$ |

**Table 4** Standard deviation of BSM models from the SM, event numbers are weighted.

### 3.5 Limitations

There are certain limitations to our study. Indeed, our VBS signal could be polluted by hidden background processes which involve di Z boson's and dijet production without an on-shell Higgs Boson's production. However, these backgrounds usually have low cross sections, although they do have an influence. Also, we decided to ignore the potential background $pp > \text{Z}jj$ since no events resulted in dijet and four lepton production out of 30 000 generated, however, we could have missed a process with a significant cross section which was not generated. Future studies could try to segment background processes further.

In the search for the most accurate selection cuts for maximum efficiency, machine learning could be used. Indeed, our selection cuts were not determined using neural networks. They could, however, be used to refine our selection cuts or identify new parameters to improve our efficiency in isolating VBF and VBS. Using machine learning is a potential route for better efficiency.

Also, our exploration of sensitivity limits is confined to VBF and only studies the effects of modification on the H-W-W vertex. Future studies could analyse other processes such as VBS and use EFT models which affect other vertices such as H-Z-Z or quartic gauge boson couplings.

## 4 Conclusion

By making use of the selection cuts $|\Delta\eta_{jj}| > 2.5$ and $m_{jj} > 200$ GeV as well as keeping within or outside of the lepton range $110 < m_{l+l-l+l-} < 130$ GeV, we can both simultaneously and separately isolate VBF and VBS. As such, one can run these selection cuts in an LHC experiment to target these processes, rich in Higgs boson and vector boson couplings. This would allow a precise measurement of the Higgs coupling with vector boson's. Any deviations from the values predicted by the SM or deviations in data distributions presented in this paper would point towards new physics, modelled by EFTs which are part of BSM theories. We also quantified exactly how BSM physics would affect the observables of our experiment by establishing a sensitivity limit of our selection cuts for H-W-W couplings for VBF. This analysis would help in BSM physics detection in future LHC analyses revolved around VBF Higgs production. Conducting an experiment at the LHC revolving around VBF and VBS, using selection cuts on the parameters we discussed could therefore be particularly useful to understand the Higgs boson and search for BSM physics.

## 5 Acknowledgments

Many thanks to Gaetano Barone, physicist at CERN, without his guidance I could not have produced this paper. Many thanks also to all the team at CERN working on simulation programs such as MadGraph5, as well as the pioneers of the past who built the foundation of the knowledge we have nowadays on the Higgs Boson.

## References

1 S. L. Glashow, *Nucl. Phys.*, 1961, **22**, 579.

2 S. Weinberg, *Phys. Rev. Lett.*, 1967, **19**, 1264.

3 A. Salam, *Elementary Particle Theory: Relativistic Groups and Analyticity*, Almqvist & Wiksell, 1968, p. 367.

4 G. 't Hooft and M. Veltman, *Nucl. Phys. B*, 1972, **44**, 189.

5 ATLAS Collaboration, *Observation of a new particle in the search for the Standard Model Higgs boson with the ATLAS detector at the LHC*, https://arxiv.org/abs/1207.7214, 2012.

6 CMS Collaboration, *Observation of a new boson at a mass of 125 GeV with the CMS experiment at the LHC*, https://arxiv.org/abs/1207.7235, 2012.

7 F. Englert and R. Brout, *Phys. Rev. Lett.*, 1964, **13**, 321.

8 P. W. Higgs, *Phys. Lett.*, 1964, **12**, 132.

9 P. W. Higgs, *Phys. Rev. Lett.*, 1964, **13**, 508.

10 G. S. Guralnik, C. R. Hagen and T. W. B. Kibble, *Phys. Rev. Lett.*, 1964, **13**, 585.

11 P. W. Higgs, *Phys. Rev.*, 1966, **145**, 1156.

12 T. W. B. Kibble, *Phys. Rev.*, 1967, **155**, 1554.

13 CERN, *SM Higgs Branching Ratios and Total Decay Widths*, https://twiki.cern.ch/twiki/bin/view/LHCPhysics/CERNYellowReportPageBR, Accessed: 2025-06-28.

14 M. Tanabashi *et al.*, *Phys. Rev. D*, 2018, **98**, 030001.

15 CMS Collaboration, *Measurement of vector boson scattering and constraints on anomalous quartic couplings from events with four leptons and two jets in proton-proton collisions at sqrt(s) = 13 TeV*, https://arxiv.org/abs/1708.02812, 2017.

16 D. Naegels, *An introduction to Goldstone boson physics and to the coset construction*, https://arxiv.org/abs/2110.14504, 2021.

17 ATLAS Collaboration, *Test of CP-invariance of the Higgs boson in vector-boson fusion production and in its decay into four leptons*, https://arxiv.org/pdf/2304.09612, 2023.

18 CMS Collaboration, *Measurements of inclusive and differential cross sections for the Higgs boson production and decay to four-leptons in proton-proton collisions at $\sqrt{s} = 13$ TeV*, https://arxiv.org/abs/2305.07532, 2023.

19 CMS Collaboration, *Measurement of vector boson scattering and constraints on anomalous quartic couplings from events with four leptons and two jets in proton-proton collisions at $\sqrt{s} = 13$ TeV*, https://arxiv.org/abs/1708.02812, 2017, Duplicate of entry CMSVBS2017.

20 *MadGraph5 aMC@NLO*, https://launchpad.net/mg5amcnlo, Accessed: 2025-06-28.

21 *PYTHIA 8.313*, https://www.pythia.org/, Accessed: 2025-06-28.

22 J. de Favereau, C. Delaere, P. Demin, A. Giammanco, V. Lematre, A. Mertens and M. Selvaggi, *JHEP*, 2014, **02**, 057.

23 *Geant4*, https://geant4.web.cern.ch/about/, Accessed: 2025-06-28.

24 *Phys. Lett. B*, 1993, **307**, 187–193.

25 C. Anastasiou, C. Duhr, F. Dulat, E. Furlan, T. Gehrmann, F. Herzog, A. Lazopoulos and B. Mistlberger, *High precision determination of the gluon fusion Higgs boson cross-section at the LHC*, https://arxiv.org/abs/1602.00695, 2016.

26 CERN, *Vector Boson Fusion Process*, https://twiki.cern.ch/twiki/bin/view/LHCPhysics/LHCHWGVBF#VBF_Calculation_for_YR4, Accessed: 2025-06-28.